



# Investigation of the cyan phosphor $\text{Ba}_2\text{Zr}_2\text{Si}_3\text{O}_{12}:\text{Eu}^{2+}, \text{Dy}^{3+}$ : Mechanoluminescence properties and mechanism

Xiaoyan Fu <sup>a, \*\*</sup>, Shenghui Zheng <sup>a</sup>, Junpeng Shi <sup>b</sup>, Yanan Liu <sup>a</sup>, Xiangyu Xu <sup>a</sup>, Hongwu Zhang <sup>b, \*</sup>

<sup>a</sup> College of Materials Science and Engineering, Key Laboratory of Functional Materials and Applications of Fujian Province, Xiamen University of Technology, Xiamen 361024, China

<sup>b</sup> Institute of Urban Environment, Chinese Academy of Sciences, Xiamen 361021, China



## ARTICLE INFO

### Article history:

Received 21 March 2018  
Received in revised form  
24 June 2018  
Accepted 29 June 2018  
Available online 30 June 2018

### Keywords:

Mechanoluminescence  
Persistent luminescence  
Traps related  
Mechanical properties

## ABSTRACT

In this paper, we have developed a cyan mechanoluminescence material  $\text{Ba}_2\text{Zr}_2\text{Si}_3\text{O}_{12}:\text{Eu}^{2+}, \text{Dy}^{3+}$  via a solid-state reaction. The crystal structure, photoluminescence and mechanoluminescence (ML) of this phosphor have been systematically investigated. The results showed that the ML intensity increased with  $\text{Dy}^{3+}$  concentration from 0.5 to 3 at.% and then reduced following a further increase in  $\text{Dy}^{3+}$  content. In addition, the maximum ML intensity was obtained for  $\text{Ba}_2\text{Zr}_2\text{Si}_3\text{O}_{12}:\text{0.02Eu}^{2+}, \text{0.03Dy}^{3+}$ . In particular, the ML spectrum was similar to the PL and afterglow emission spectra with a slight red shift, showing a dominant peak at approximately 508 nm that was generated from the 5d-4f transition of  $\text{Eu}^{2+}$ . Furthermore, when the decay time was less than 1 h, the ML intensity rapidly decreased following an increase in the load circle. Following an increase in decay time, the ML intensity was stable and was hardly affected by the load circles. The thermoluminescence (ThL) results have shown that the addition of  $\text{Dy}^{3+}$  can create three types of traps with trap depths of 0.682, 0.742 and 0.79 eV. Through combination of the ML and ThL results, the ML mechanism can be explained by the detrapping process of the electrons in shallow and deep traps that were induced by piezoelectricity. The relation between the ML intensity and compressive stress was nearly linear in the test range, indicating that the sample can be used as sensors to detect stress. Furthermore, a cyan ML light can clearly be observed by the naked eye in the dark, which suggested that  $\text{Ba}_2\text{Zr}_2\text{Si}_3\text{O}_{12}:\text{Eu}^{2+}, \text{Dy}^{3+}$  can visualize the stress in an object.

© 2018 Elsevier B.V. All rights reserved.

## 1. Introduction

Mechanoluminescence (ML) materials can achieve mechano-optical conversion under external mechanical stimuli, such as compression, impact and friction [1–3]. A large number of studies have revealed that ML phosphors present an accurate linearity of emission intensity against external loads [4–6], which can be used as ML sensors to detect stress in an object. Furthermore, via the utilization of a CCD imager, ML sensors can realize in situ and in time visualization of the stress distribution [7]. Due to these advantages, until now, ML sensors have attracted increasing attention, with applications in areas such as safety monitoring; crack

detection in bridges, tunnels, and gas vessels; and the identification of personal handwriting by dynamic pressure mapping [8–10]. To date, many ML materials with different luminescent colors, such as  $\text{SrMg}_2(\text{PO})_4:\text{Eu}^{2+}$  (blue) [11],  $\text{BaSi}_2\text{O}_2\text{N}_2:\text{Eu}^{2+}$  (bluish-green) [12],  $\text{SrAl}_2\text{O}_4:\text{Eu}^{2+}$  (green) [1],  $\text{ZnS}:\text{Mn}$  (yellow) [13],  $\text{CaZnOS}:\text{Mn}$  (orange) [14],  $\text{Sr}_{n+1}\text{Sn}_n\text{O}_{3n+1}:\text{Sm}^{3+}$  (reddish-orange) [15] and  $(\text{Ba},\text{Ca})\text{TiO}_3:\text{Pr}^{3+}$  (red) [2], have been explored. However, as a novel luminescent phenomenon, there remains a general lack of understanding of the ML mechanism, which has limited the development of ML materials. Thus, a detailed exploration of the ML mechanism is necessary for the further development of more efficient ML materials.

Currently, many studies have been performed to elucidate the ML mechanism, and several possible ML models have been established. However, some conflicts still exist for these models. Chandra suggested that the ML that originated from the strain-induced thermal energy (thermoluminescence) and strain-induced electric

\* Corresponding author.

\*\* Corresponding author.

E-mail addresses: [fuxiaoyan@xmut.edu.cn](mailto:fuxiaoyan@xmut.edu.cn) (X. Fu), [hwzhang@iue.ac.cn](mailto:hwzhang@iue.ac.cn) (H. Zhang).

field (electroluminescence) produced by the movement of dislocations [16,17], while the studies of Xu have shown that trapped electrons in ML materials have an important effect on the ML [6]. The obscure ML mechanism was not advantageous for the development of ML materials. It is well known that  $\text{Eu}^{2+}$  ions have been an efficient activator for various luminescent modes, including photoluminescence, persistent luminescence, electroluminescence and mechanoluminescence. A large number of studies have provided abundant information regarding the energy level and various luminescent mechanisms of  $\text{Eu}^{2+}$ , indicating that  $\text{Eu}^{2+}$  ion-doped luminescent materials are suitable models for the exploration of novel luminescent mechanisms [1,18,19]. Thus, the development of high-efficiency  $\text{Eu}^{2+}$ -doped ML materials is advantageous to further understand the ML mechanism.

Here, a cyan ML material  $\text{Ba}_2\text{Zr}_2\text{Si}_3\text{O}_{12}:\text{Eu}^{2+}, \text{Dy}^{3+}$  was developed. Furthermore, various co-dopant contents of  $\text{Dy}^{3+}$  affected the number of traps and then induced a change in the ML intensity. Additionally, the structure of  $\text{Ba}_2\text{Zr}_2\text{Si}_3\text{O}_{12}$  was easily investigated via X-ray Rietveld refinement, which provided detailed information regarding the crystal unit cell. In this way,  $\text{Ba}_2\text{Zr}_2\text{Si}_3\text{O}_{12}:\text{Eu}^{2+}, \text{Dy}^{3+}$  was an excellent research model to systematically investigate the ML mechanism. Thus, in this paper, we have developed  $\text{Ba}_2\text{Zr}_2\text{Si}_3\text{O}_{12}:\text{Eu}^{2+}, \text{Dy}^{3+}$  with various concentrations of  $\text{Dy}^{3+}$  ions and then studied its ML mechanism via a combination of persistent luminescence, mechanoluminescence and thermoluminescence.

## 2. Experimental section

### 2.1. Synthesis of $\text{Ba}_2\text{Zr}_2\text{Si}_3\text{O}_{12}:\text{Eu}^{2+}, \text{Dy}^{3+}$

In our experiments,  $\text{Ba}_{2-x}\text{Zr}_2\text{Si}_3\text{O}_{12}:\text{Eu}^{2+}, \text{xDy}^{3+}$  (where  $x = 0.005, 0.01, 0.02, 0.03$  and  $0.05$ ) ML materials were prepared in a high-temperature solid-state reaction from a stoichiometric mixture of  $\text{Ba}(\text{NO}_3)_2$  (99.999%),  $\text{ZrO}_2$  (AR),  $\text{SiO}_2$  (AR),  $\text{Eu}_2\text{O}_3$  (99.99%), and  $\text{Dy}_2\text{O}_3$  (AR). The mixture of raw materials was ground thoroughly in an agate mortar with ethanol for 30 min, and the mixed powder was preheated at  $800^\circ\text{C}$  for 2 h in air conditions. Then, the as-prepared materials were ground again for 10 min, and the obtained mixture was sintered in alumina crucibles under a  $\text{H}_2$  flow (5%  $\text{H}_2$ , 95% Ar) atmosphere at  $1450^\circ\text{C}$  for 6 h. Finally, the prepared samples were cooled to room temperature and reground for further measurements.

### 2.2. Material characterization

The crystal phases of the as-prepared powders were characterized by using X-ray diffraction (XRD) in the  $2\theta$  range from  $10^\circ$  to  $75^\circ$  (PANalytical X'Pert PRO with  $\text{Cu K}\alpha$  radiation;  $\lambda = 1.5405980 \text{ \AA}$ ; tube voltage, 40 kV; current, 40 mA). The surface morphologies of the samples were analyzed by transmission electron microscopy (TEM) (FEI Talos F200S) with an energy-dispersive X-ray accessory. The photoluminescence (PL) and persistent luminescence properties of as prepared powder were recorded by using an Edinburgh FLS920 instrument with a 450 W xenon lamp and an M300 monochromator. For evaluating the ML properties of the samples, composite pellets (diameter, 25 mm; thickness, 15 mm) were prepared by mixing the  $\text{Ba}_2\text{Zr}_2\text{Si}_3\text{O}_{12}:\text{Eu}^{2+}, \text{Dy}^{3+}$  powders with an optical epoxy resin, wherein the mass of powder to resin is 1:2. The pellets were exposed to UV light (365 nm) for 2 min, and the ML intensity under the load was measured after different times with a lab-built system that comprises a universal testing machine (AG-X, Shimadzu) and a photocounting system, which consisted of a photomultiplier tube (55777, Ortel Instruments), and a photometer (C9692, Hamamatsu). In addition, the ML images were recorded by a complementary metal oxide semiconductor camera

(D7000, Nikon). Thermoluminescence (ThL) glow curve experiments were performed using a nitrogen bath cryostat (Optistat DN, Oxford Instruments) and a temperature controller (Intelligent temperature controller, Oxford Instruments). The ThL glow curves were recorded with a linear heating rate of 10 K/min. For each sample, 50 mg powder was employed. Prior to the measurements, the powder was also exposed to a mercury lamp at a 365 nm wavelength for 2 min and different delay times (5 min, 10 min, 20 min and 1 h, 4 h, 8 h). Then, the thermoluminescence was measured at 504 nm from 270 to 500 K. All the measurements were performed at room temperature except for the ThL curve measurements.

## 3. Results and discussions

### 3.1. Structure analysis of $\text{Ba}_2\text{Zr}_2\text{Si}_3\text{O}_{12}:\text{Eu}^{2+}, \text{Dy}^{3+}$

The structure of  $\text{Ba}_2\text{Zr}_2\text{Si}_3\text{O}_{12}:\text{Eu}^{2+}, \text{Dy}^{3+}$  was investigated via the XRD patterns and Rietveld refinement, as shown in Fig. 1. Note that the diffraction peaks (Fig. 1 (a)) of the all the samples were similar and can be indexed to the standard reference pattern of  $\text{Ba}_2\text{Zr}_2\text{Si}_3\text{O}_{12}$  (JCPDS No. 025-1466), indicating that the  $\text{Eu}^{2+}$  and  $\text{Dy}^{3+}$  ions have been incorporated into the  $\text{Ba}_2\text{Zr}_2\text{Si}_3\text{O}_{12}$  host lattice with no impurities. To gain further detailed crystallographic information regarding the prepared samples, the  $\text{Ba}_2\text{Zr}_2\text{Si}_3\text{O}_{12}:\text{Eu}^{2+}, \text{Dy}^{3+}$

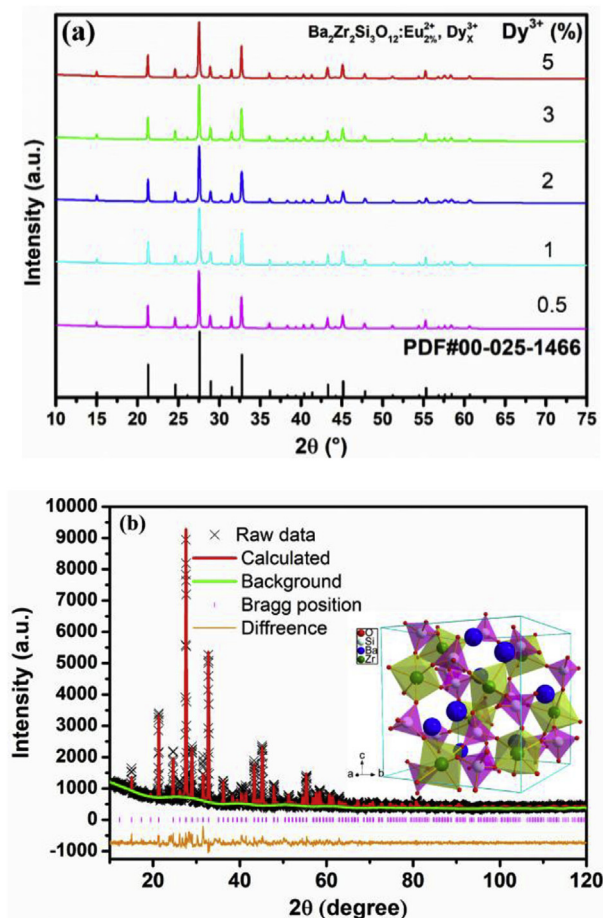


Fig. 1. (a) XRD patterns of the  $\text{Ba}_2\text{Zr}_2\text{Si}_3\text{O}_{12}:\text{Eu}^{2+}, \text{xDy}^{3+}$  ( $x = 0.005, 0.01, 0.02, 0.03, 0.05$ ) samples. X increases from the bottom to the top. (b) Rietveld refinement of  $\text{Ba}_2\text{Zr}_2\text{Si}_3\text{O}_{12}:\text{Eu}^{2+}, \text{Dy}^{3+}$  prepared at  $1450^\circ\text{C}$ , and the inset photograph shows the crystal structure of  $\text{Ba}_2\text{Zr}_2\text{Si}_3\text{O}_{12}$ , which was drawn on the basis of the Rietveld refinement results.

Download English Version:

<https://daneshyari.com/en/article/7990356>

Download Persian Version:

<https://daneshyari.com/article/7990356>

[Daneshyari.com](https://daneshyari.com)